Applicability of Resonance Forms in Pyrimidinic Bases. An AIM Study

María J. González Moa[†,‡] and Ricardo A. Mosquera*[,‡]

Departamento Química Orgánica and Departamento Química Física, Universidade de Vigo, Lagoas-Marcosende, 36200-Vigo, Galicia, Spain

Received: February 21, 2003; In Final Form: April 21, 2003

The applicability of resonance theory to explain the protonation of pyrimidinic bases was analyzed within the framework of the atoms in molecules (AIM) theory using B3LYP/6-31++G**//B3LYP/6-31G** charge densities of the neutral and diverse protonated forms of uracil and cytosine. The present study demonstrates that AIM atomic properties and delocalization indexes do not follow the trends that should be expected according to the resonance model. The resonance model is only able to predict the stability sequence of protonated forms and explain the changes exhibited by most of the bond properties upon protonations. Both the O- and N-protonated forms are found to be better described by $RO-H^+$ and $RN-H^+$ forms than by the classical RO^+-H and RN^+-H structures. According to the AIM analysis the electron charge gained by the proton is mainly provided by the other hydrogens of the molecule.

Introduction

Some derivatives of pyrimidinic bases have been found as potent drugs in the management of cancer. One of the most interesting is 5-fluoruracil, which has been used in the treatment of colorectal cancer for the previous 40 years.[1] Also, new oral fluoropyrimidines appear to be at least as active and with less toxicity, improved quality of life, and less expense.[2] Thus, the development and rationalization of pyrimidil-based strategies for the treatment of cancer[2] has promoted the interest on pyrimidinic compounds.

The applicability of the resonance model to explain the structure and reactivity of organic compounds has been generally accepted[3,4] and has been proved as a very useful tool in chemistry. Nevertheless, some facts obtained from topological analysis of charge densities carried out with the atoms in molecules (AIM) theory are not keeping in line with the predictions provided by the resonance model. Thus, Wiberg and Laidig computed the atomic populations of several conformations of formic acid, methyl formate, acetic acid, and methyl acetate and found them inconsistent with the resonance model.[5] The need of the resonance model to explain the hindered rotation within amides was also questioned.[5,6] Later, Laidig and Cameron found that the delocalization of π charge density from nitrogen to sulfur in thioamides was negligible.[7] Also, it has been recently found that the resonance model does not describe correctly the charge distribution in the protonated forms of linear[8,9] and cyclic[10] aliphatic ethers.

The AIM theory[11,12] allows the partitioning of a molecule into disjoint subsystems without resorting to hypotheses alien to quantum mechanics. With a few exceptions,[13] each of these subsystems consists of a nucleus, which acts as an attractor for the trajectories of the gradient of the charge density vector field, $\nabla\rho(\mathbf{r})$, and its associated atomic basin, throughout which these trajectories spread. An atom, Ω, is defined as the union of the attractor and its associated basin, and is surrounded by zero flux surfaces for $\nabla\rho(\mathbf{r})$. The integration of the proper density functions within these limits provides diverse atomic properties such as the electron population, $N(\Omega)$, or the total atomic electron energy, $E(\Omega)$. AIM theory also recovers main elements of molecular structure in terms of the critical points, $\mathbf{r}_c$, of the electron charge density, $\rho(\mathbf{r})$. Prominent among these points is the bond critical point (BCP), which is located roughly between two bonded atoms.

Thus, the AIM theory provides very useful tools to analyze the effects due to any chemical change experienced by a molecule. It has been used to study the effects produced by diverse substitutions,[14,15] conformational effects,[16,17] dimer formation,[18,19] bond formation and dissociation,[20] and protonation.[8−10,21,22]

No AIM study has been carried out on the protonation of pyrimidinic bases, despite their interest, the simplicity of the theoretical treatment required, and the potential of such study to give an insight into the role of resonance forms in these aromatic heterocycles. Therefore, we have performed AIM calculations on the neutral and protonated forms of uracil and cytosine aiming to compare the evolution of atomic and bond properties experienced by these systems upon protonation with the predictions provided for them by the resonance model.

Computational Details

B3LYP/6-31++G**//B3LYP/6-31G** full optimizations were carried out for the neutral and protonated forms of uracil (**1**) and cytosine (**2**) using the Gaussian98 program.[23] All optimized structures were characterized as minima in the frequency calculation. The AIM atomic and bond properties were calculated using the AIMPAC[24] and MORPHY[25,26] programs on those charge densities. We observed that the error in the determination of the interatomic surfaces of the carbonyl carbons, measured by $L(\Omega)$,[11] was substantially reduced when the integrations were performed considering the existence of second and third intersections between every integration ray and those interatomic surfaces.

Virial ratios differed from 2 in less than 9.6×10^{-3}. Integration errors expressed as differences between total proper-

* To whom correspondence should be addressed. E-mail: mosquera@uvigo.es.
† Departamento Química Orgánica.
‡ Departamento Química Física.

10.1021/jp034451s CCC: $25.00
Published on Web 06/13/2003

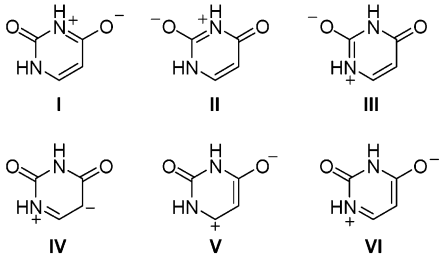

Figure 1. Main resonance forms of uracil.

ties and those obtained by summation of properties of the fragments [$N - \sum N(\Omega)$ or $E - \sum E(\Omega)$] were always smaller (in absolute value) than 3.6×10^{-3} au and 2.7 kJ/mol, respectively. The summations of the integrated values of the Laplacian of the charge density in all the atomic fragments [$\sum L(\Omega)$] were always smaller (in absolute value) than 4.6×10^{-3} au. The discrepancies in the additivity of atomic charges and energies from their molecular counterparts were found to be accurate enough compared with other works carried out at similar theoretical levels.

Results and Discussion

Delocalization in the Neutral Forms. The delocalization indexes, $\delta(A,B)$, introduced by Bader et al.[27−29] and defined by eq 1 from the integration of the density of the Fermi hole on two atomic basins A and B, provide a measure of the number of electrons shared or exchanged between those atoms. $F(A,B)$ in eq 1 (numerically equal to $F(B,A)$) is the total Fermi correlation integrated for basin A due to the electron charge in basin B, and $S_{ij}(A)$ denotes the overlap of a pair of i, j occupied spin−orbitals over atom A.

$$\delta(A,B) = |F(A,B) + F(B,A)| = 2\sum_i \sum_j S_{ij}(A)\, S_{ij}(B) \quad (1)$$

These indexes were successfully employed to provide a quantitative representation of the resonance structures of conjugated and aromatic hydrocarbons.[27] Values obtained for these indexes in pyridine have also shown that the inclusion of an electronegative heteroatom gives rise to substantial modifications in the delocalization of aromatic heterocycles with regard to that presented by aromatic hydrocarbons.[27] The number of electronegative heteroatoms in pyrimidinic bases points to expectation of even larger modifications that could override the qualitative description of delocalization obtained from their resonance structures. Thus, we have computed $\delta(A,B)$ indexes for molecules **1** and **2**. If electron delocalization is described correctly by the resonance structures (Figures 1 and 2), we should only find significant $\delta(A,B)$ values between nonbonded atoms for those pairs of atoms that bear a charge in one of those resonance structures, namely, N3−O10, N3−O8, N1−O8, N1−C5, C6−O10, and N1−O10 for uracil (molecule numbering is detailed in Figure 3). The corresponding $\delta(A,B)$ values could be employed to measure, respectively, the weight of the resonance structures I−VI; i.e., form I is represented by δ(N3,O10).

Table 1 contains the $\delta(A,B)$ values larger than 0.02 au that correspond to pairs of nonbonded atoms. It can be observed that the largest δ values in **1** correspond to the resonance forms I−IV. Nevertheless, surprisingly, δ values related to forms V and VI are even smaller than those corresponding to electron delocalizations not represented by any of the traditional resonance forms (i.e., δ(C5,O10), δ(N1,N3)), or are in the same range as indexes involving hydrogen atoms (δ(C6,H11), δ(C5,H12), or δ(N1,H12)).

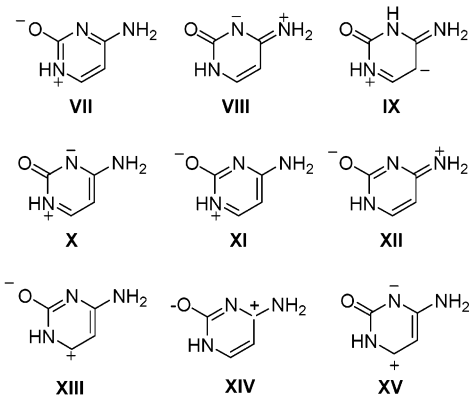

Figure 2. Main resonance forms of cytosine.

For cytosine, the largest $\delta(A,B)$ values correspond to resonance forms VII−XI. However, there are some high δ values that do not correspond to electron delocalizations represented by any of the traditional resonance forms (i.e., δ(N3,O8), δ(C5,N9), or δ(N3,C5)). Also, resonance form XII is not supported by a high δ value. In fact, δ(O8,N9) (0.015 au) is equivalent to the δ index observed between hydrogens 10 and 11.

Though in strict sense a density of the Fermy hole cannot be defined within the density functional formalism, the numerical values obtained for δ (A, B) indexes with the Kohn−Sham spin orbitals (Table 1) are very similar to those calculated with HF wave functions.

The plane of symmetry in **1** and **2** allows the calculation of σ and π delocalization indexes. The values obtained for π delocalization indexes, $\delta^{\pi}(A,B)$ (Table 1), indicate that (a) π delocalization is substantially smaller than what is generally expected and in most cases the largest contribution to $\delta(A,B)$ corresponds to σ delocalization, and (b) though the largest $\delta^{\pi}(A,B)$ values correspond to some resonance forms, there are still $\delta^{\pi}(A,B)$ values unrelated to any classic resonance form that exceed those of other resonance structures.

Protonation Processes. Table 2 displays the calculated B3LYP/6-31++G** energies for the neutral and diverse protonated forms of uracil (**1**) and cytosine (**2**). Nomenclature of protonation sites is shown in Figure 3. The reliability of the computational level here used is supported by a good agreement with experimental proton affinities (PA)[30] (discrepancies are less than 19 kJ mol^{-1}).

Despite the limitations related above for the description of the electron delocalization, the resonance model still predicts correctly the preferred sites of protonation. Thus, (a) the most stable protonated forms for each compound according to our B3LYP calculations (**1f**+/**1e**+, **2c**+/**2b**+) are those that can be written with the largest number of resonance structures (forms I, V, and VI of Figure 1 and forms VII and XI−XIV of Figure 2), (b) **2d**+ is the unique N-protonated species with comparable stability to the O-protonated forms, and (c) protonated forms where it is not possible to write any resonance form (**1a**+, **1d**+, **2a**+, **2e**+) are destabilized by more than 75 kJ mol^{-1}.

Good linear relationships between E(H) and N(H) are found for N- and O-protonations. Nevertheless, it has to be stressed that PAs, contrary to what had been found for a set of carbonyl groups,[22] are not linearly correlated with electron population or the electronic energy in the proton basin. This points to the presence of significantly different electron charge distortions in the molecule for the diverse protonations. Whereas for alkyl

TABLE 1: Total, $\delta(A,B)$, and π, $\delta^{\pi}(A,B)$, Delocalization Indexes for Neutral Uracil and Cytosine (in au)[a]

	$\delta(A,B)$							$\delta^{\pi}(A,B)$				
	N1	C2	N3	C4	C5	C6		N1	N3	C4	C5	C6
						Molecule **1**						
N3	0.132						N3	0.042				
C4	0.029						C4	0.021				
C5	0.148	0.020	0.083				C5	0.098	0.021			
C6		0.020	0.033	0.076			C6		0.024	0.039		
O8	0.235		0.242		0.027		O8	0.096	0.110	0.005	0.026	0.005
O10	0.030		0.255		0.131	0.058	O10	0.028	0.108		0.043	0.046
H11				0.033		0.053						
H12	0.064				0.048							
						Molecule **2**						
N3	0.135						N3	0.035				
C4	0.045	0.029					C4	0.033				
C5	0.157	0.024	0.091				C5	0.104	0.030			
C6		0.021	0.062	0.075			C6		0.053	0.037		
O8	0.241		0.231	0.030	0.031		O8	0.090	0.099	0.018	0.030	0.005
N9	0.024		0.233		0.102	0.029	N9	0.022	0.116		0.038	0.021
H12				0.036		0.052						
H13	0.067				0.047							

[a] Values less than 0.02 au and those corresponding to pairs of bonded atoms are not shown.

TABLE 2: Total Energies, *E*, Vibrational Energy Corrections, ZPVE, Proton Affinities (Experimental Values in Parentheses), PA, and Main Atomic Properties of the Proton for Diverse Forms of the Compounds Studied Here (Figure 1)[a]

molecule	*E* [au]	ZPVE [kJ/mol]	PA [kJ/mol]	*N*(H) [au]	*E*(H) [au]
1	**−414.847 43**	229.2			
1a+	**−415.129 97**	260.4	710.5	0.495	−0.4036
1b+	**−415.167 55**	260.5	809.1	0.341	−0.3173
1c+	**−415.169 82**	261.5	814.1	0.337	−0.3145
1d+	**−415.137 34**	258.7	731.6	0.494	−0.4008
1e+	**−415.180 82**	262.4	842.0	0.351	−0.3230
1f+	**−415.185 59**	263.2	853.8 (872.7)	0.342	−0.3190
2	**−394.963 29**	257.5			
2a+	**−395.307 32**	288.7	872.0	0.514	−0.4160
2b+	**−395.325 86**	294.4	915.0	0.366	−0.3342
2c+	**−395.339 78**	296.3	949.6 (949.9)	0.343	−0.3175
2d+	**−395.339 21**	296.0	948.4	0.507	−0.4114
2e+	**−395.287 65**	295.3	813.7	0.499	−0.4038

[a] All properties were calculated from B3LYP/6-31++G**//B3LYP/6-31G** charge densities.

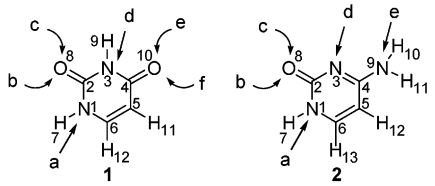

Figure 3. Protonations and atom numbering in uracil (**1**) and cytosine (**2**).

ketones PA values display an excellent linear correlation with the charge of the C═O group,[31,32] even the qualitative sequence of computed PAs for the diverse protonation sites in a pyrimidinic base cannot be explained by the atomic electron charges of the neutral molecule. Thus, *N*(O8) (9.215 au) is larger than *N*(O10) (9.193 au) in uracil, and N3 presents the smallest electron population of the nitrogens in cytosine (8.177 au compared to 8.237 au at N1 and 8.254 au at N9). PAs are also not correlated with the corresponding values of $-\nabla^2\rho(\mathbf{r})$ at its (3,−3) critical points that indicate the protonation sites.

O^+-H vs $O-H^+$ Structures. According to the AIM description, the proton maintains a very high charge in all the protonated species. O-protonation gives rise to lower electron charge donations to the proton (between 0.337 and 0.366 au) than N-protonation (between 0.494 and 0.514 au) (Table 2). All the O-protonations give rise to a slight decrease (never larger than 0.101 au) of the electron population of the corresponding oxygen, O^{α} (Table 3). This reduction results from a larger increase of π electron population and a substantial reduction of σ population—both facts completely unexpected according to the resonance model (Tables 4 and 5). Despite the electron population reduction, O^{α}, far from bearing a positive charge, still presents a significantly high negative charge (always higher than −1.1 au), in contrast to the strongly positive charge on the attached proton. This suggests that O-protonated forms are better described by an $O-H^+$ structure than by the widespread O^+-H structure,[3] as was recently found in cyclic[10] and linear ethers[8,9] and in linear ketones.[32] The same trends can be concluded from the results obtained by Slee and Bader at the HF/6-31G* level for diverse carbonyl compounds.[22]

The properties exhibited by the $O-H^+$ bond in all the O-protonated forms are quite similar to those presented by the hydroxylic bond in 1-alkanols.[17] In fact, the largest differences are as unmeaningful as a 1% displacement in the relative position of the BCP and a reduction of 0.014 au in $\rho(\mathbf{r}_c)$. It is also noticeable that *N*(O) in the O-protonated forms is only around 0.14 au less than that of an *n*-alkanol.

According to the AIM description, only 17%−28% of the electronic population acquired by the proton is reduced in the O^{α} basin, whereas most of that charge is lost by atoms separated from the proton by more than two bonds (Table 3). Surprisingly, the electron population of the neighboring carbonylic carbon, C^{β}, increased in all cases. δ indexes computed for the protonated

TABLE 3: Absolute Values, $N(\alpha)$, and Variations with Regard to the Neutral Form, $\Delta N(\alpha)$, of the Atomic Electron Population of the Protonated Atom[a]

	α atom	$N(\alpha)$	$N^0(\alpha)$	$\Delta N(\alpha)$	$\sum\Delta N(\beta)$	$\sum\Delta N(\mathrm{H})$	$\sum\Delta N(\nu)$
1a+	N1	8.048	8.253	−0.205	0.275	−0.256	−0.307
1b+	O8	9.136	9.215	−0.079	0.020	−0.223	−0.055
1c+	O8	9.139	9.215	−0.076	0.020	−0.227	−0.049
1d+	N3	7.996	8.201	−0.205	0.030	−0.233	−0.084
1e+	O10	9.128	9.193	−0.065	0.185	−0.230	−0.239
1f+	O10	9.136	9.193	−0.057	0.180	−0.225	−0.240
2a+	N1	8.266	8.237	0.029	−0.357	−0.198	0.011
2b+	O8	9.121	9.222	−0.101	0.023	−0.253	−0.033
2c+	O8	9.150	9.222	−0.072	0.066	−0.280	−0.057
2d+	N3	8.217	8.177	0.040	−0.095	−0.293	−0.161
2e+	N9	8.086	8.254	−0.168	0.205	−0.313	−0.227

[a] $N^0(\alpha)$ represents the corresponding electron population at the neutral molecule. Values are given for the summations of the variations experienced by atoms in β to the proton, $\sum\Delta N(\beta)$, the remaining hydrogens in the molecule, $\sum\Delta N(\mathrm{H})$, and the rest of atoms, $\sum\Delta N(\nu)$. All values in au.

TABLE 4: Variations (au Multiplied by 10^3) in the Total, $\Delta N(\Omega)$, and π, $\Delta N^\pi(\Omega)$, Atomic Electron Population in the O-Protonated Forms of Uracil[a]

	$\Delta N(\Omega)$				$\Delta N^\pi(\Omega)$			
atom	**1b**+	**1c**+	**1e**+	**1f**+	**1b**+	**1c**+	**1e**+	**1f**+
C2	*20*	*20*	10	1	*29*	*28*	7	5
C4	9	31	*185*	*180*	4	8	*66*	*66*
C5	−51	−49	−75	*−47*	−93	−82	−5	24
C6	55	31	*−109*	*−129*	21	3	*−124*	*−135*
H7	−31	−54	−50	−50	−3	−4	−4	−4
H9	−54	−34	−33	−55	−4	−3	−3	−4
H11	−70	−70	−69	−42	−8	−8	−5	−3
H12	−67	−70	−78	−78	−3	−4	−7	−7
N1	*15*	*18*	*−13*	*−15*	*−22*	*−35*	*−67*	*−73*
N3	*−10*	*−11*	*18*	*23*	*−59*	*−48*	*−28*	*−39*
O8	−79	−76	−70	−73	196	196	−63	−67
O10	−73	−69	−65	−57	−66	−59	225	228

[a] $\Delta N(\Omega)$ and $\Delta N^\pi(\Omega)$ values that should be expected to be negative according to the resonance model are in italics.

TABLE 5: Variations (au Multiplied by 10^3) in the Total, $\Delta N(\Omega)$, and π, $\Delta N^\pi(\Omega)$, Atomic Electron Population in the O-Protonated Forms of Cytosine[a]

	$\Delta N(\Omega)$		$\Delta N^\pi(\Omega)$	
	2b+	**2c**+	**2b**+	**2c**+
C2	*2*	*−18*	*36*	*28*
C4	*−13*	*2*	*−19*	*−15*
C5	−61	−58	−92	−83
C6	*37*	*17*	*−4*	*−18*
H7	−27	−55	−2	−3
H10	−41	−37	−4	−4
H11	−48	−49	−5	−5
H12	−69	−68	−10	−9
H13	−69	−72	−4	−4
N1	*32*	*43*	*−1*	*−14*
N3	−9	22	−30	−8
N9	*0*	*0*	*−83*	*−78*
O8	−101	−72	208	207

[a] $\Delta N(\Omega)$ and $\Delta N^\pi(\Omega)$ values that should be expected to be negative according to the resonance model are in italics.

forms also indicate that no important delocalization takes place between the proton and atoms not directly bonded to it. In fact, none of these δ values represents more than 2% of the total electron population of the proton basin, while the summation of proton autocorrelation index and $\delta(\mathrm{H},\mathrm{O}^\alpha)$ accounts for more than 95% of the proton electron population. All these facts indicate that protonation gives rise to a global modification of the charge distribution that cannot be reduced to the displacement of π electron pairs located on certain atoms or bonds.

According to the AIM results the nitrogen atom bonded to the proton keeps, in all cases, a significant negative charge (7.996 in **1d**+ is the lowest N(N) value). δ values between the proton and atoms not bonded to it are very small (each one of these δ values represents less than 2% of the electronic population). Again the traditional resonance mechanism to explain the protonation leaving a positive charge on the nitrogen atom is not supported by the topological electron charge analysis.

Modification of Atomic and Bond Properties upon Protonation. It is a well-known fact that both atomic and bond properties of a neutral molecule are significantly altered by protonation. It could be expected that these changes should be important (or at least noticeable) in a wider region of the molecule when it presents significant delocalizations. Thus, protonation on a certain atom *A* related by electron delocalization to another atom *B* results in modifications of both the *A* and *B* atomic properties, i.e., both $N(A)$ and $N(B)$. When the *A*,*B* delocalization can be represented by a classical resonance form related to the main Lewis structure by the displacement of double bonds, protonation should also give rise to significant variations of BCP properties of those bonds.

Changes on Atomic Properties upon O-Protonation.

As was described above, protonations **1f**+ and **1e**+ are related to resonance forms I, V, and VI; protonations **1b**+ and **1c**+ are related to resonance forms II and III; and protonations **2b**+ and **2c**+ are related to resonance forms VII and XI−XIV. Thus, resonance theory predicts $N(\Omega)$ reductions on atoms N1, N3, and C6 for **1e**+ and **1f**+, N1 and N3 for **1b**+ and **1c**+, and N1, N9, C4, and C6 for **2b**+ and **2c**+. Surprisingly, AIM computed $\Delta N(\Omega)$ values (Tables 4 and 5) do not follow the resonance model predictions. Thus, we observe positive $\Delta N(\Omega)$ values for N1 in **1b**+ and **1c**+ and for N3 in **1e**+ and **1f**+. Also, we can observe that the most important variations in the atomic electron population (if we exclude the atom to which the proton is attached) are exhibited by other atoms where no

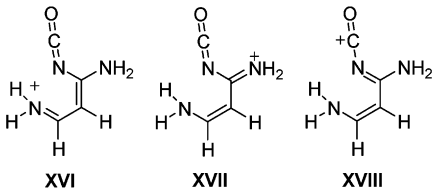

Figure 4. Main resonance forms of **2a**+ protonated form of cytosine.

TABLE 6: Main BCP Properties for the 2a+ Protonated Form of Cytosine (All Values but ϵ in au)

bond	$10^2\epsilon$	R	$10^2\rho(\mathbf{r}_c)$
N3−C4	3.6	2.602	30.3
C4−N9	25.6	2.530	34.1
C4−C5	27.7	2.645	31.1
C5−C6	18.7	2.633	31.1
N9−H10	4.5	1.908	34.2
N9−H11	4.3	1.910	34.1
C5−H12	4.9	2.046	28.6
C6−H13	1.1	2.054	29.5

charge is located by any resonance form (O10, H11, H12, H9, and C5 in **1b**+/**1c**+; C4, O8, H11, H12, C5, and H7 in **1e**+/**1f**+; H12, H13, and C5 in **2b**+/**2c**+).

We have also integrated separately π and σ charge densities in order to test if variations of π atomic electron population, $\Delta N^{\pi}(\Omega)$ (Tables 4 and 5), keep in line with the predictions of the resonance model, as was previously found in benzene derivatives.[33,34] It can be observed that if we exclude Cα atoms, $\Delta N^{\pi}(\Omega)$ presents the expected sign (according to the resonance model) for all atoms where resonance forms leave charges. Nevertheless, the absolute value of these variations is really small when we compare them with the $\Delta N^{\pi}(\Omega)$ values shown by other atoms. For instance, in **1b**+, ΔN^{π}(N1) only achieves −0.022 au, whereas ΔN^{π}(C5) and ΔN^{π}(O10) respectively reach −0.093 and −0.066 au. In cytosine we can also compare ΔN^{π}(N1) = −0.001 au with ΔN^{π}(C5) = −0.092 au.

All these results lead us to conclude that the resonance model does not provide an adequate representation of the electron charge modifications experienced by uracil and cytosine upon O-protonation.

Variation of Atomic Properties upon N-Protonation.

Uracil can experience two N-protonations (**1a**+ and **1d**+, Figure 1), **1d**+ being the most stable (Table 1). It must be noticed that the carbon atoms bonded to the nitrogen gain more electron charge than that taken from the protonated nitrogen (Table 3). The electron population of the rest of the molecule is reduced approximately in the same amount obtained by the proton.

Cytosine can experience three N-protonations: **2a**+, **2d**+, and **2e**+ (Figure 3). The conformer obtained for the first form presents an open chain structure (Figure 4). It displays a very positive charge at C2. The δ indexes for this structure indicate that, contrary to what could be expected, there is no important electron charge delocalization between O8 and N1 ($\delta = 0.008$); that can be considered negligible compared to δ(N3,O8) = 0.353. On the contrary, important delocalizations are found between atoms not related by resonance forms, i.e., δ(C5,N9) = 0.135. BCP properties of **2a**+ are consistent with an important accumulation of double bonds, with big ϵ values for C5−C6, C4−C5, and C4−N9. This trend is also confirmed by their bond lengths (Table 6). This fact is in line with a combination of resonance forms XVI−XVIII (Figure 8) that, once more, are not supported by variations of AIM atomic electron populations.

The most stable N-protonated form of cytosine, **2d**+, is stabilized (according to the resonance model) by structures VIII, X, and XV, due to a delocalization of the positive charge on N3 over N9, N1, and C6, respectively. Nevertheless, we observe that the electron population of N3 is substantially increased (0.040 au), that of N1 increases in 0.008 au, N(N9) decreases very slightly (−0.003 au), and only N(C6) decreases substantially (−0.033 au). The trend predicted by the resonance model is also not followed by $\Delta N^{\pi}(\Omega)$ values (though we found a large decrease of π electron population at C6 and slight decreases at N1 and N9, N^{π}(N3) increases 0.244 au).

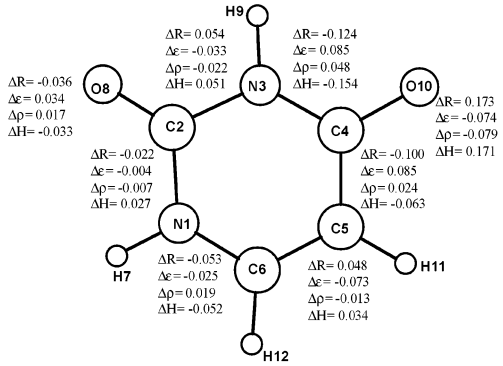

Figure 5. Variations experienced by BCP properties in **1f**+ protonation. All values, but ϵ, in au.

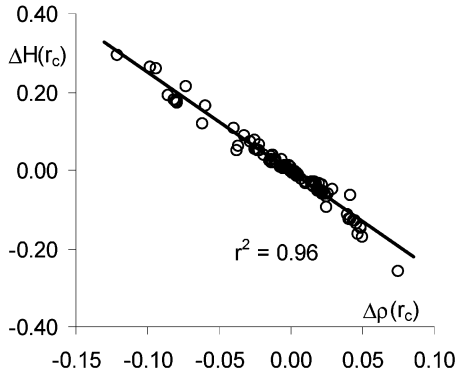

Figure 6. Plot of variations experienced by $H(\mathbf{r}_c)$ vs $\rho(\mathbf{r}_c)$ in all protonations considered in this work. Similar plots can be obtained for R vs $\rho(\mathbf{r}_c)$ ($r^2 = 0.94$) and ϵ vs $\rho(\mathbf{r}_c)$ (though $r^2 = 0.61$ there is a fairly good qualitative relationship).

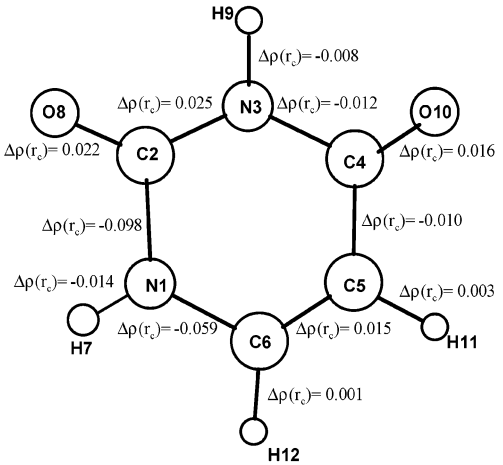

Figure 7. Variations experienced by $\rho(\mathbf{r}_c)$ in protonations **1b**+ and **1c**+. All values in au.

Changes on BCP Properties upon O-Protonation.

The most favored protonation of uracil, **1f**+, gives rise to significant modifications of the BCP properties. The variations exhibited by the C4═O10 BCP properties (Figure 5) indicate a

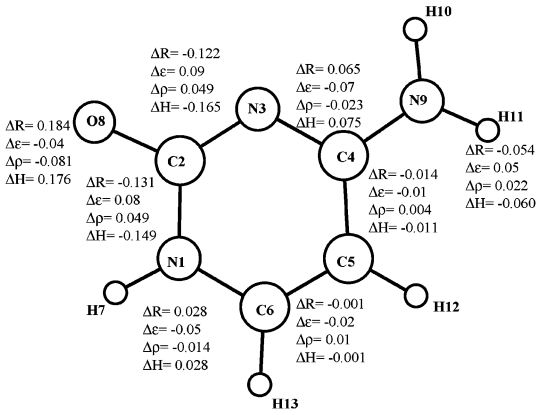

Figure 8. Variations experienced by BCP properties in **2b**+ and **2c**+ protonations. All values, but ϵ, in au.

significant reduction in the bond strength (lower $\rho(\mathbf{r}_c)$ and longer bond length) and in its covalent character (less negative $H(\mathbf{r}_c)$). The reduction experienced by $\nabla^2\rho(\mathbf{r}_c)$ (data not shown) is not meaningful because of the previously demonstrated proximity of C═O BCP to a nodal surface for $\nabla^2\rho(\mathbf{r})$.[35] The variations experienced by the BCP properties of the remaining bonds (Figure 4) can be explained by taking into account the formation and disappearance of double bonds in resonance forms I−VI (Figure 1). Thus, $\rho(\mathbf{r}_c)$ and ϵ values are reinforced (while R and $H(\mathbf{r}_c)$ are depleted) for single bonds transformed into double bonds when writing structures that leave a negative charge on O10 (I, V and VI) and are diminished for double bonds transformed into single bonds in the same structures. The only bond where the resonance structures produce conflicting trends is N1−C6. We observe that $\rho(\mathbf{r}_c)$ increases and ϵ decreases for this bond. None of the BCP properties of **1e**+ differ significantly from those in **1f**+.

The variations introduced by protonation on the remaining BCP properties can be related to those experienced by $\rho(\mathbf{r}_c)$ (Figure 6); thus in what follows we will refer only to the latter.

The evolution of BCP properties in protonations **1b**+ and **1c**+ (Figure 7) is in good agreement with resonance forms II and III (Figure 1). Thus, $\rho(\mathbf{r}_c)$ values increase for N1−C2 and C2−N3 and reduce for C2═O8. There are also slight variations for N1−C6 and N3−C4 that indicate these bonds get weaker, which can be explained as a consequence of the favored delocalization of the nitrogen lone pair over the oxygen atom. In the same direction and with the same interpretation, a slight effect is also noticeable in C4═O10, whereas the remaining bonds do not experience any significant change.

The interpretation of the evolution of BCP properties in **2b**+ and **2c**+ protonations (Figure 8) from the resonance model should be done considering the structures VII, XI, XII, XIII, and XIV. All of them agree with the reduction of C2═O8 $\rho(\mathbf{r}_c)$ (−0.083 au). Nevertheless, we observe that the evolution of BCP properties in these compounds is inconsistent with those forms. Thus, the increase experienced by C2−N3 $\rho(\mathbf{r}_c)$ could only be explained considering forms XI, XII, and XIV. Form XI is the only one supported by a significant δ index (δ(N1,O8) = 0.241), whereas the corresponding δ indexes for forms XII and XIV, respectively, δ(O8,N9) and δ(C4,O8), are very small. Finally, form XI is inconsistent with the reduction experienced by N1−C6 $\rho(\mathbf{r}_c)$ (Figure 8).

Also, the resonance model does not explain why BCP variations at C2−N3 ($\Delta\rho(\mathbf{r}_c) = 0.049$ au) are twice those found at N3−C4 ($\Delta\rho(\mathbf{r}_c) = -0.023$ au) and C4−N9 ($\Delta\rho(\mathbf{r}_c) = 0.022$ au). This fact could be explained taking into account the delocalization indicated by δ(N3,O8) that is not represented by a classical resonance form.

Variation of Bond Properties upon N-Protonation.

We observe in **1d**+ and **1a**+ that $\rho(\mathbf{r}_c)$ is depleted in all the N−Cα bonds, whereas it is reinforced in α−β bonds and decreases again, though slightly, for β−γ bonds (Figure 6). That is, BCP properties display in N-protonated forms (where there are not any resonance forms) a behavior similar to that found in O-protonations (where this behavior could be interpreted by using resonance forms).

For **2d**+ the variation of $\rho(\mathbf{r}_c)$ values experienced by some bonds can be explained by using the resonance forms VIII, X, and XV: increase at C4−N9, decrease at N3═C4, and negligible variations for N1−C6, C5═C6, and C4−C5. On the contrary, N1−C2, C2═O8, and C2−N3 display variations that cannot be related to any resonance form. However, the modifications observed in this part of the molecule could be expected taking into account the large value presented by δ(N3,O8) (Table 1).

Conclusions

The atomic and bond properties, and the delocalization indexes, calculated within the framework of the AIM theory for the neutral and protonated forms of uracil and cytosine have been used to assess the applicability of resonance forms in order to analyze chemical properties in pyrimidinic bases. It has been demonstrated that, whereas the evolution of the bond properties after protonation can be partially explained by using resonance forms, the atomic electron populations and δ delocalization indexes are inconsistent with those forms.

As was previously pointed out for other oxygenated compounds, the O-protonated forms of pyrimidinic bases are better represented by O−H$^+$ structures than by the widely used O$^+$−H forms. Thus, (1) the charge gained by the proton is taken from the rest of the molecule (especially by the other hydrogens), and (2) the oxygen atom, far from losing the electron population gained by the proton, can even display larger electron populations in the protonated form than in the neutral one. Also, δ indexes for the proton and those atoms not directly bonded to it never represent more than 2% of the total electron population in the proton basin.

The above trends can be extended to N-protonations. In these cases, the nitrogen atoms display always substantially negative charges in the protonated forms, whereas the hydrogen atoms bonded to them present an electron population around 0.5 au.

Acknowledgment. Helpful discussions with Prof. C. Terán and Prof. A. M. Graña are deeply acknowledged. We are also indebted to Prof. R. F. W. Bader for providing us a copy of AIMPAC package of programs.

References and Notes

(1) Marshall, J. L. In *Colorectal Cancer*; Saltz, L. B., Ed.; Humana Press Inc.: Totowa, NJ, 2002; p 499.
(2) Ignoffo, R. J. *Am. J. Health-Syst. Pharmacy* **1999**, *56*, 2417.
(3) Carey, F. A.; Sundberg, R. J. *Advanced Organic Chemistry*; Kluwer Academic: New York, 2001.
(4) Wheland, G. W. *Resonance in Organic Chemistry*; Wiley: New York, 1955.
(5) Wiberg, K. B.; Laidig, K. E. *J. Am. Chem. Soc.* **1987**, *109*, 5935.
(6) Wiberg, K. B.; Breneman, C. M. *J. Am. Chem. Soc.* **1992**, *114*, 831.
(7) Laidig, K. E.; Cameron, L. M. *J. Am. Chem. Soc.* **1996**, *118*, 1737.
(8) Vila, A.; Mosquera, R. A. *J. Phys. Chem. A* **2000**, *104*, 12006.
(9) Vila, A.; Mosquera, R. A. *Chem. Phys. Lett.* **2000**, *332*, 474.
(10) Vila, A.; Mosquera, R. A. *Tetrahedron* **2001**, *57*, 9415.

(11) Bader, R. F. W. *Atoms in Molecules: A Quantum Theory*; Oxford University Press: New York, 1990.
(12) Bader, R. F. W. *Chem. Rev.* **1991**, *91*, 893.
(13) Cioslowski, J. *J. Phys. Chem.* **1990**, *94*, 5496.
(14) Wiberg, K. B.; Breneman, C. M. *J. Am. Chem. Soc.* **1990**, *112*, 8765.
(15) Wiberg, K. B. *J. Org. Chem.* **1991**, *56*, 544.
(16) González Moa, M. J.; Terán, C.; Mosquera, R. A. *Int. J. Quantum Chem.* **2002**, *86*, 67.
(17) Mandado, M.; Graña, A. M.; Mosquera, R. A. *Chem. Phys. Lett.* **2002**, *355*, 529.
(18) Caroll, M. T.; Bader, R. F. W. *Mol Phys.* **1988**, *65*, 695.
(19) Koch, U.; Popelier, P. L. A. *J. Phys. Chem.* **1995**, *99*, 9747.
(20) Hernández Trujillo, J.; Bader, R. F. W. *J. Phys. Chem. A* **2000**, *104*, 1779.
(21) Stutchbury, N. C. J.; Cooper, D. L. *J. Chem. Phys.* **1983**, *79*, 4967.
(22) Slee, T.; Bader, R. F. W. *J. Mol. Struct. (THEOCHEM)* **1992**, *255*, 173.
(23) Frisch, M. J.; Trucks, G. W.; Schlegel, H. B.; Scuseria, G. E.; Robb, M. A.; Cheeseman, J. R.; Zakrzewski, V. G.; Montgomery, J. A., Jr.; Stratmann, R. E.; Burant, J. C.; Dapprich, S.; Millam, J. M.; Daniels, A. D.; Kudin, K. N.; Strain, M. C.; Farkas, O.; Tomasi, J.; Barone, V.; Cossi, M.; Cammi, R.; Mennucci, B.; Pomelli, C.; Adamo, C.; Clifford, S.; Ochterski, J.; Petersson, G. A.; Ayala, P. Y.; Cui, Q.; Morokuma, K.; Malick, D. K.; Rabuck, A. D.; Raghavachari, K.; Foresman, J. B.; Cioslowski, J.; Ortiz, J. V.; Stefanov, B. B.; Liu, G.; Liashenko, A.; Piskorz, P.; Komaromi, I.; Gomperts, R.; Martin, R. L.; Fox, D. J.; Keith, T.; Al-Laham, M. A.; Peng, C. Y.; Nanayakkara, A.; Gonzalez, C.; Challacombe, M.; Gill, P. M. W.; Johnson, B. G.; Chen, W.; Wong, M. W.; Andres, J. L.; Head-Gordon, M.; Replogle, E. S.; Pople, J. A. *Gaussian 98*; Gaussian, Inc.: Pittsburgh, PA, 1998.
(24) Bader, R. F. W.; et al. *AIMPAC: A suite of programs for the AIM theory*; McMaster University, Hamilton, Ontario, Canada L8S 4M1. Contact bader@mcmail.cis.mcmaster.ca.
(25) Popelier, P. L. A.; with contribution from Bone, R. G. A. *MORPHY98, a topological analysis program*; UMIST: Manchester, England.
(26) Popelier, P. L. A. *Chem. Phys. Lett.* **1994**, *288*, 160.
(27) Bader, R. F. W.; Streitwieser, A.; Neuhaus, A.; Laidig, K. E.; Speers, P. *J. Am. Chem. Soc.* **1996**, *118*, 4959.
(28) Fradera, X.; Austen, M. A.; Bader, R. F. W. *J. Phys. Chem. A* **1999**, *103*, 304.
(29) Bader, R. F. W.; Matta, C. F. *Inorg. Chem.* **2001**, *40*, 5603.
(30) Hunter, E. P.; Lias, S. G. *J. Phys. Chem. Ref. Data* **1998**, *27*, 413.
(31) Graña, A. M.; Mosquera, R. A. *Chem. Phys.* **1999**, *243*, 17.
(32) Mosquera, R. A.; Graña, A. M. *Recent Res. Dev. Chem. Phys.* **2001**, *2*, 23.
(33) Bader, R. F. W.; Chang, C. *J. Phys. Chem.* **1989**, *93*, 2946.
(34) Bader, R. F. W.; Chang, C. *J. Phys. Chem.* **1989**, *93*, 5095.
(35) Hwang, T.-S.; Wang, Y. *J. Phys. Chem. A* **1998**, *102*, 3726.